



## The Use of Resistance Sensors to Measurement of Shape Charge Parameters

Adam WIŚNIEWSKI

*Military Institute of Armament Technology,  
7 Wyszyńskiego St., 05-220 Zielonka, Poland  
E-mail: adam.wisniewski@witu.mil.pl*

**Abstract:** In the article different methods of measurement of the collapsing liner parameters and the formation of the shape charge jet by resistance sensor which was placed inside the shape charge are presented. The speed and acceleration change while reducing of resistance sensor length for shape charge in casing and without it for the different angles of the shape charge liner is analyzed. The resistance sensor placed in the shape charge liner permitted to register the parameters which cannot be obtained by the X-ray impulse apparatus. By the resistance sensor placed at the angle to the shape charge axis or perpendicular to the internal surface of the shape charge liner, the reducing shape charge liner parameters were registered. The resistance sensor placed on the shape charge axis enabled to register the parameters of the jet forming in the shape charge. In case of placing of resistance sensor on shape charge casing, the graphs become more stable in comparison with the graphs obtained when resistance sensor was placed inside shape charge.

**Keywords:** sensors, shape charge, explosives, shape charge jet

### Introduction

In the experiments with shape charge it is essential problem to recognize the reducing liner shape charge parameters and the parameters of shape charge jet forming [1-6]. This permits to recognize the influence of the elements shape charge parameters on the creation of shape charge jet process and makes it possible to obtain the shape charge with very high abilities to perforate rolled homogeneous armour, RHA.

It is the best to carry out the measuring of the reducing liner parameters by the multi-lamp X-ray impulse apparatus, which registers the following phases of the liner and jet movement on the photographic plate. From these photos it can qualify the reduction of each fragment of the liner speed and their change of impact angle on the  $x$  axis during time and space. Because of the lack of such apparatus, the substitute research, which relies on the continuous measurement of the reducing liner speed, using resistance change of the shortening resistance sensor, was carried out [1-4]. The scheme of this meter circuit is shown in Figure 1.

The resistance change of this sensor is registered by the storage oscilloscope, the screen of which was then photographed. The 0.2 mm diameter resistance sensor was placed at the different angles of the axis (different value  $y_p$ ) – for the registering speeds of the liner elements along the axis  $X'$  and when it was placed along the axis  $x$  of shape charge, then the speed of the shape charge jet front was examined. The resistance sensor was soldered on to the liner top or it was glued to the liner top.

The difficulties of these measurements were connected with the necessity of electromagnetic disturbances elimination, when the wires were too long. When the experiments were carried out in the bunker and the registering apparatus was behind its wall, the disturbances' influence on the measurement results was smaller. The second factor making these tests difficult was the use of the very quick storage oscilloscope with the high sensitivity of the input entrance which was very vulnerable to the electromagnetic disturbances.

Before the measurements every resistance sensor was calibrated. The influence of air shock wave on the registration phenomenon processes of the sensors covered and not covered with lacquer were examined. No difference between the registered phenomenon graphs of the resistance sensors was found. It means that, the moving liner or the shape charge jet (when  $y_p=0$ ) decides about the shortening of the resistance sensor but not the air shock wave.

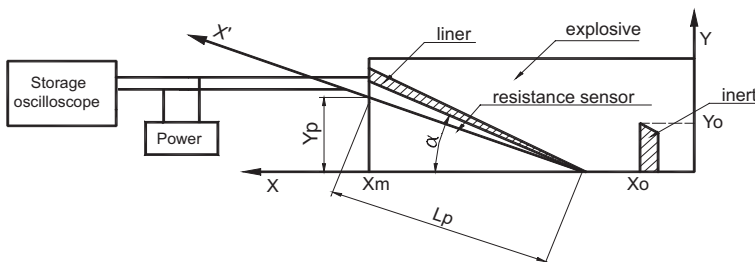


**Figure 1.** The registering apparatus scheme for testing of the liner reduction process.

In the registering apparatus (Figure 1) the value of the power supply current of the resistance sensor was changed and its obtained optimum value was 1 A. The correctness of the obtained results depended on quality of this sensor and on elimination of electric disturbances, thermoelectric SEM and of shock and electromagnetic wave, generated during the explosion. The resistance sensors were made from different alloys and different lengths. Each of them was made in the several versions: (stranded with different jump with enamel copper wire, resisting and copper wires were placed in parallel, resisting wire was either enamel covered or not). The resistance sensor was bent at the  $c_1$  distance of its beginning. It caused starting the registration process of the sensor resistance changes from the certain threshold value, resulting from the length of the bent sensor. It made the registration of the first movement of the shape charge liner elements easy because the high jump of the tension was registered by oscilloscope [5, 6].

## Testing results

Different kinds of the resistance sensors were placed in different places of shape charges, i.e. along the shape charge axis (Figure 2a), at the variable angles of this axis (Figure 2b), perpendicular to the surface of the liner (Figure 2c) and on the surface of the shape charge casing (Figure 2d).

The testing results of the liner reduction process according to Figure 2a are presented in Figures 3 and 8, according to Figure 2b they are presented in Figures 4 and 9 also 5 and 10, according to Figure 2c they are presented in Figures 6 and 11 but according to Figure 2d the testing results are presented in Figure 7 and Figure 12.

All the tests results presented in Figures 8-12 were carried out on the basis of the oscilloscope photos (Figure 3-7) by the CODIMAT device. For this purpose the program was worked out, which guaranteed appropriate accuracy of the photos processing, their approximation and smoothing of the curves. This program enabled carrying out the speed  $V$  and accelerations a graph. In order to observe the little changes, the speed scale  $V$  was stretched and the speed  $V$  value was limited only to  $8500 \text{ m s}^{-1}$ .

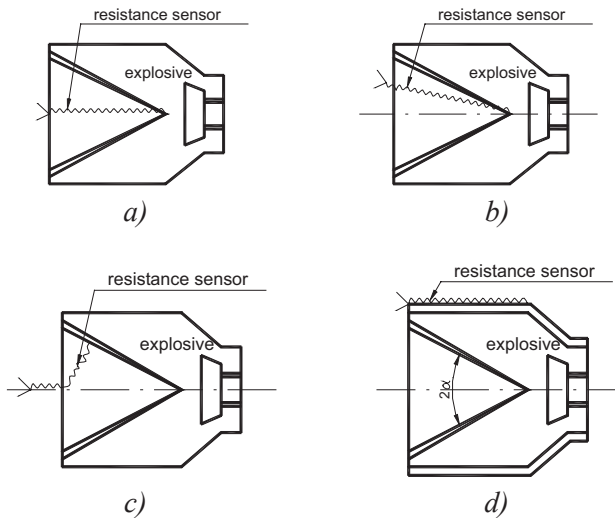


**Figure 2.** The location scheme of the resistance sensors in the different places of the shape charges: a) along of the shape charge axis; b) at the angle different from the decline angle of liner to the shape charge axis; c) - perpendicularly to the liner surface; d) on the surface of the shape charge casing.

After starting the program, the  $x$  and  $y$  coordinate values of the select points on the graph were found. The minimum number of the selected points should not be smaller than 100, however, more these points gives a more extract curve. The points' values on the graph can be store in computer manually with the (1-2) mm step or it is done automatically with the appropriate  $t$  time or  $x$  distance step.

The tests according to Figure 2a were carried out for PG-7WM shape charge warhead without ballistic cap with the diameter of 70.5 mm. The obtuse angle of the shape charge liner is  $2\alpha=60^\circ$ . The length of the used resistance sensor was  $l=80$  mm and its bend  $c_f=10$  mm. The results of this test are presented in Figure 3 and Figure 8. The graph of ( $x$ ) length change of shortening resistance sensor is presented on the oscillogram (Figure 3) as linear and continuous one. Small oscillations can be seen only in the central part of this graph.

The length change  $X$  of the shortening resistance sensor, placed on the shape charge axis, and the change of the speed  $V$  and the acceleration  $a$  in time  $t$  function of the registration phenomenon are presented in Figure 8. The change of the shortening resistance sensor length  $X$  has almost linear character. However the speed  $V$  of this resistance sensor shortening during the time up to  $4 \mu\text{s}$  is about  $(6500-8500) \text{ m s}^{-1}$ . Whereas later, it sharply decreases to the value about

$1000 \text{ m s}^{-1}$ . Because of the scarce computer smoothing of this graph it contains many peaks. The acceleration  $a$  of the registered process while  $3 \mu\text{s}$  has the stable character and it is about zero, but from  $(3-7) \mu\text{s}$  is about  $a = (-8000-2000) \text{ m s}^{-2}$ .

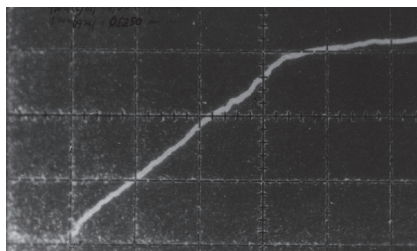


**Figure 3.** Tension change in time function in resistance sensor placed on axis of PG-7WM shape charge without ballistic cap (Figure 2a,  $y_p=0$ ,  $c_l=10 \text{ mm}$ ).

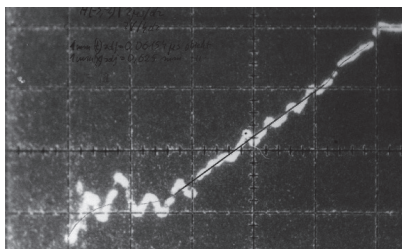


**Figure 4.** Tension change in time function in resistance sensor placed on  $X'$  axis of shape charge model without casing (Figure 1, 2b,  $y_p=25 \text{ mm}$ ,  $c_l=5 \text{ mm}$ ).

The following tests according to Figure 2b were carried out for the model: shape charge without casing [6, 7], with the diameter of about  $66 \text{ mm}$ , the obtuse angle of the shape charge liner  $2\alpha=40^\circ$ , the length of the resistance sensor bending  $c_l=5 \text{ mm}$  ( $y_p=25 \text{ mm}$  – Figure 1) and for PG-7WM shape charge without ballistic cap, and the length of resistance sensor bending  $c_l=10 \text{ mm}$  ( $y_p=25 \text{ mm}$  – Figure 1). The results of these experiments are presented in Figures 4, 9, 5, 10.

On the oscillogram (Figure 4) the graph of length change  $X$  of shortening resistance sensor is clearly unstable. The greatest deviations are in the first graph part, however in the farther part they get smaller but do not disappear.

The character of the length changing  $X$  of the shortened resistance sensor while  $2.5 \mu\text{s}$ , presented in Figure 9, is hardly stable. While  $(2.5-6) \mu\text{s}$  the graph of these changes is exactly linear and later minor instabilities appear. Reflection of the unstable flight of the shape charge liner elements in its first stage are the

very impetuous changes of the shortening resistance sensor speed  $V$ . During stable flight of the liner elements, the speed of the shortened resistance sensor does not have the high changes and it is about  $(7000-7500) \text{ m s}^{-1}$ . The acceleration  $a$  in the first phase of registration (up to  $3.5 \mu\text{s}$ ) is limited  $a=(-7500-5000) \text{ m s}^{-2}$  and while  $3.5-6 \mu\text{s}$  it again has the big changes of value.

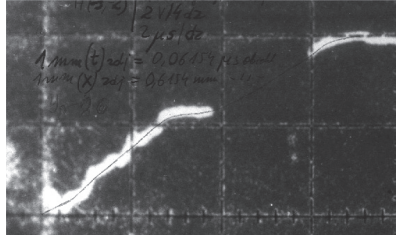


**Figure 5.** Tension change in time function in resistance sensor placed on X' axis (Figure 1) of PG-7WM shape charge without ballistic cap (Figure 1, 2b,  $y_p=25 \text{ mm}$ ,  $c_l=10 \text{ mm}$ ).

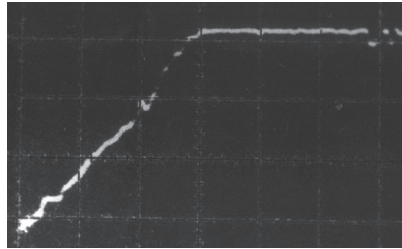


**Figure 6.** Tension change in time function in resistance sensor placed perpendicularly to the internal surface of liner of shape charge model (Figure 2c,  $y_p=0$ ,  $c_l=10 \text{ mm}$ ).

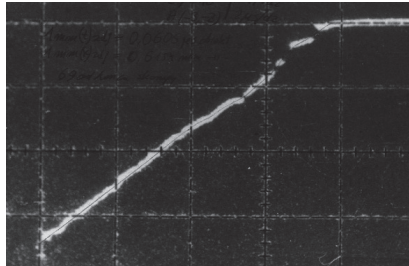


**Figure 7.** Tension change in time function in resistance sensor placed on the casing surface of shape charge model (Figure 2d,  $c_l=10 \text{ mm}$ ).

On the oscillogram (Figure 5) quite stable changes of length  $X$  of resistance sensor can be observed but in the central part of a registered phenomenon there are large pauses. In Figure 10 the change of the resistance sensor length  $X$  up to  $3.5 \mu\text{s}$  is almost linear, but later the resistance sensor length  $X$  is shortened fast. Reflection of this graph character is the very big variability of the speed  $V$  in the limits of  $(6500-8500) \text{ m s}^{-1}$  and of the acceleration  $a$ .

The tests according to Figure 2c were carried out by the resistance sensor of the length  $l=95 \text{ mm}$  ( $c_l=10 \text{ mm}$ ) placed perpendicularly to the internal surface of the liner of model shape charge without casing. The obtained graphs are shown in Figure 6 and Figure 11.

As it can be seen in Figure 6, there is the large pause in the recording of length change  $X$  of shortening resistance sensor. Beside this, this graph is stable and impetuous peaks do not exist.

During the time  $t=2 \mu\text{s}$ , the  $X$  length change of shortening resistance sensor is linear (Figure 11), then it changes and during  $t=(3.5-5) \mu\text{s}$  again is linear. The result of this is the  $V$  speed changing of the elements flight of the shape charge liner, which in the first phase has the value of about  $V=(7000-8500) \text{ m s}^{-1}$ , next it drops to the values about  $2000 \text{ m s}^{-1}$  and again it achieves the value of about  $6500 \text{ m s}^{-1}$ . The graph of the acceleration  $a$  is unstable and it hesitates in the limits of  $(3000-4500) \text{ m s}^{-2}$ .

The last kind of the tests were carried out (Figure 2d) for the model shape charge in the casing with the use of resistance sensor of the length  $l=70 \text{ mm}$  ( $c_l=10 \text{ mm}$ ) placed on the shape charge casing. The results of these tests are presented in Figure 7 and Figure 12.

On the last oscillogram (Figure 7) the graph of length  $X$  change of shortened resistance sensor is as follows: in the first part it is a linear one without any jumps, but in the central part there are small pauses in the registered phenomenon.

In Figure 12 the length  $X$  change of shortening resistance sensor by the time  $t=3.5 \mu\text{s}$  is almost linear, and next it has small deviations. Whereas, the graph of the liner elements speed  $V$  by the time  $t=3 \mu\text{s}$  is stable enough and it is about  $6500 \text{ m s}^{-1}$  and after this time it changes suddenly. At first the speed gets smaller to the value about  $5000 \text{ m s}^{-1}$ , and next it grows to the value about  $8500 \text{ m s}^{-1}$  and again drops almost linearly to the zero value. As a result of this the acceleration  $a$  graph by the time  $t=2.5 \mu\text{s}$  is also stable and riches the value about zero, however after this time it changes about  $a=(-5000-3000) \text{ m s}^{-2}$ .

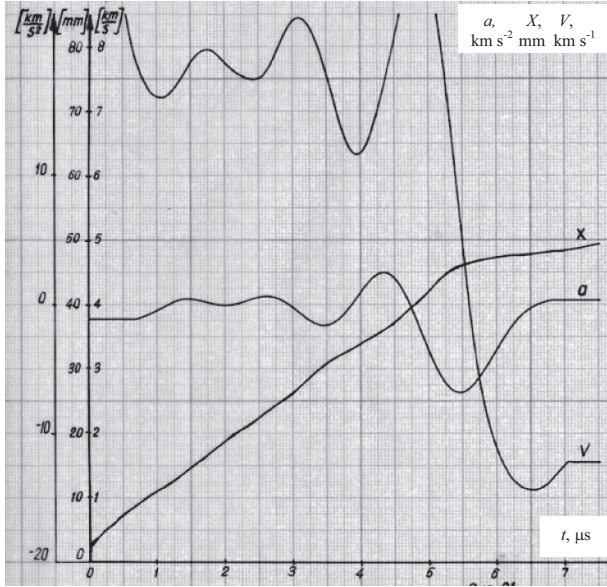


**Figure 8.** PG-7WM shape charge without ballistic cap  $y_p=0$ ,  $c_l=10$  mm. The change of the  $X$  length of the shortening resistance sensor placed on PG-7WM shape charge axis, the change of the speed  $V$  and the acceleration  $a$  in the  $t$  time function.

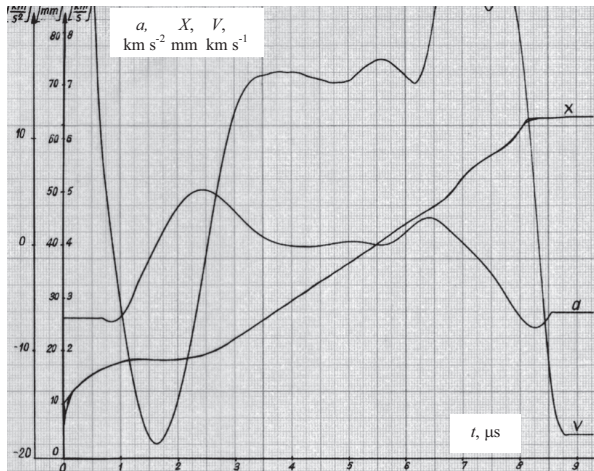


**Figure 9.** Shape charge model without casing  $y_p=25$  mm,  $c_l=5$  mm. The change of the  $X$  length of shortening resistance sensor, placed on the shape charge model  $X'$  axis (Figure 1) without casing, the change of the speed  $V$  and the acceleration  $a$  in time  $t$  function.



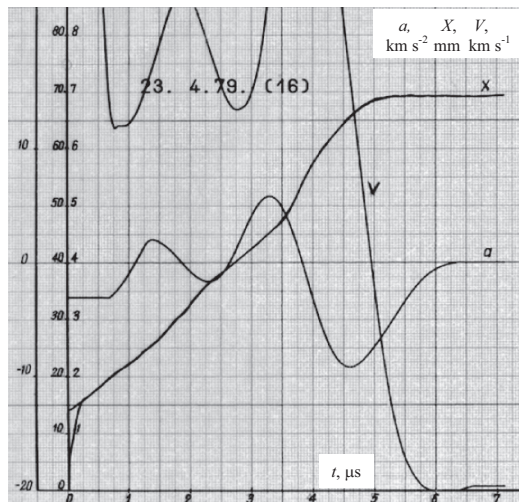


**Figure 10.** PG-7WM shape charge without ballistic cap  $y_p=25$  mm,  $c_f=10$  mm. The change of the  $X$  length of the shortening resistance sensor, placed on PG-7WM shape charge  $X'$  axis (Figure 1), the change of the speed  $V$  and the acceleration  $a$  in time  $t$  function.

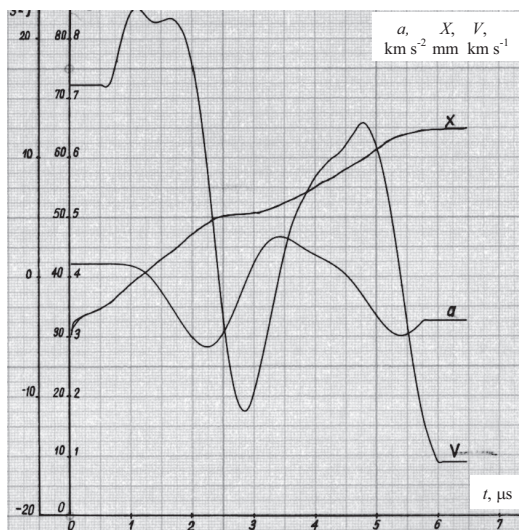


**Figure 11.** Model of the shape charge without ballistic cap  $c_f=10$  mm. The change of the  $X$  length of the shortening resistance sensor, placed perpendicularly to the interior surface of shape charge model, the change of the speed  $V$  and the acceleration  $a$  in time  $t$  function.

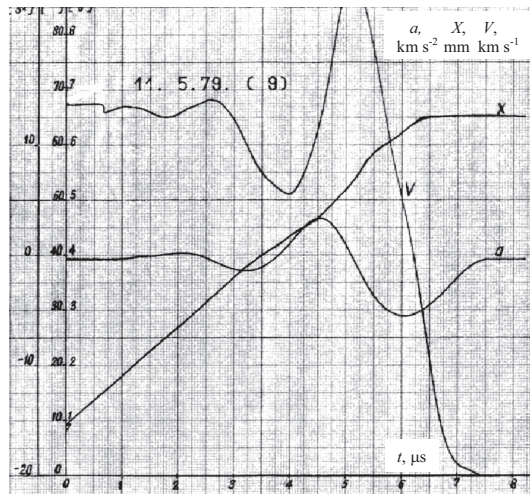


**Figure 12.** Shape charge model in casing  $c_I=10$  mm. The change of the  $X$  length of the shortening resistance sensor, placed on the shape charge model casing (Figure 2), the speed  $V$  and the acceleration  $a$  in  $t$  time function.

## Conclusions

On the basis of the tests the following conclusions can be presented:

1. The resistance sensor placed between the shape charge axis and the internal surface of the shape charge liner permits to register the parameters which could not be obtained by the X-ray impulse apparatus or the fast camera.
2. By the resistance sensor placed at an angle of the shape charge axis or perpendicularly to the internal surface of the shape charge liner, it is possible to register the parameters of the reducing shape charge liner.
3. The resistance sensor placed on the shape charge axis permits to register the parameters of the forming shape charge jet.
4. The shape charge with the liner of small obtuse angle  $2\alpha=40^\circ$  produces the shape charge jet of which the front speed and the speed of rest elements are greater than the speed of the shape charge with a big liner angle of  $2\alpha=60^\circ$ .
5. The forming of the shape charge jet of a greater speed takes place with bigger instabilities, especially in the first and the final period.
6. The liner elements' speed  $V$  of the PG-7WM shape charge in the initial flight phase at once has high values (7000-8500)  $\text{m s}^{-1}$  as distinct from the same elements of shape charge model, the speed of which decreases suddenly

below 1000 m/sec and after about 1.5  $\mu\text{s}$  obtains the value  $V=7000 \text{ m s}^{-1}$ . In case of the shape charge with the obtuse angle ( $2\alpha=60^\circ$ ) liner the speed of liner elements is greater than in case of the obtuse angle ( $2\alpha=40^\circ$ ) liner. It results from the fact that in the first case the detonation wave in the explosive of the shape charge reaches the liner elements at a greater angle (in relation to the liner surface) than in the second case. It causes propelling of these liner elements to greater speeds.

7. The maximum change of the acceleration value  $a$  of the reducing liner elements (PG-7WM shape charge) in the first period (to  $\approx 3.5 \mu\text{s}$ ) is about 3 times greater than the acceleration value of the shape charge jet forming from these elements.
8. By placing the resistance sensor in the different places of the explosive charge (on the external surface, on the casing, internal of explosive etc.), the detonation speed, the speed of the casing elements, etc., can be tested.
9. In case of placing of resistance sensor on shape charge casing, the graphs become more stable in comparison with the graphs obtained when resistance sensor was placed inside shape charge. In the first phase of the phenomenon the speed graphs  $V$  and acceleration graphs  $a$  achieve almost constant values.
10. The received graphs of the  $V$  and  $a$  parameters' values, „smoothed” slightly, permit to register the minimum changes of the  $V$  and  $a$  and the extreme values of these parameters.

## References

- [1] Bakalarski J., Madej W., Wiśniewski A., The Oscilloscope Research of the Hollow Charge by the X-Ray Apparatus and Influence of the Detected Defects on the Armour Penetration Depth, *Armament Technology and Radiolocation Problems*, WITU, Exercise book 13, **1975**.
- [2] Kupidura Z., Nowak H., Wiśniewski A., The Projecting and the Results of the Hollow Charge Research for the Single Use Grenade Launcher, *Armament Technology and Radiolocation Problems*, WITU, Exercise book 25, **1975**.
- [3] Wiśniewski A., The Research of the Energy Explosive Shaped Charge, WITU, Warsaw **1978**, not published.
- [4] Wiśniewski A., Krzyżowski Z., *The Electronic System for the Continuous Measurement of the Quick Processes Parameters*, Patent PL No 123342, **1982**.
- [5] Wiśniewski A., *Armours - Construction, Designing and Research*, Scientific and Technical Publishing House, Warsaw **2001** (in Polish).
- [6] Wiśniewski A., Żurowski W., *Ammunition and Armour*, Radom University of Technology, Radom **2001** (in Polish).

